PNAS RESEARCH ARTICLE | EVOLUTION

Genetic architecture of dispersal and local adaptation drives accelerating range expansions

Jhelam N. Deshpande[a,b,1] and Emanuel A. Fronhofer[b,1]

Edited by Marcus Feldman, Stanford University, Stanford, CA; received December 2, 2021; accepted May 31, 2022

Contemporary evolution has the potential to significantly alter biotic responses to global change, including range expansion dynamics and biological invasions. Models predicting range dynamics often make highly simplifying assumptions about the genetic architecture underlying relevant traits. However, genetic architecture defines evolvability and higher-order evolutionary processes, which determine whether evolution will be able to keep up with environmental change or not. Therefore, we here study the impact of the genetic architecture of dispersal and local adaptation, two central traits of high relevance for range expansions, on the dynamics and predictability of invasion into an environmental gradient, such as temperature. In our theoretical model we assume that dispersal and local adaptation traits result from the products of two noninteracting gene-regulatory networks (GRNs). We compare our model to simpler quantitative genetics models and show that in the GRN model, range expansions are accelerating and less predictable. We further find that accelerating dynamics in the GRN model are primarily driven by an increase in the rate of local adaptation to novel habitats which results from greater sensitivity to mutation (decreased robustness) and increased gene expression. Our results highlight how processes at microscopic scales, here within genomes, can impact the predictions of large-scale, macroscopic phenomena, such as range expansions, by modulating the rate of evolution.

gene-regulatory network | environmental gradient | biological invasion | robustness | evolvability

Significance

To predict contemporary ecological and evolutionary dynamics, one must take the speed of evolution, that is, the rates of evolutionary processes, into account. These rates depend on how variation for relevant traits is generated or eliminated, which depends on their genetic basis. Here we model range expansions into environmental gradients and use gene-regulatory networks to represent dispersal and local adaptation, two key traits for range expansions. Indeed, incorporating an explicit genetic basis for traits leads to predictions different from simpler models: particularly, gene-regulatory networks evolve greater sensitivity to mutation, increasing the rate of adaptation to the gradient. Importantly, this leads to accelerating range expansions. Our results highlight how assumptions at the genomic level modify predictions of large-scale regional processes.

Range expansions and species invasions are happening at an increasing rate as a result of human activities, such as species introductions, the rewiring of dispersal networks (1), and global changes, in general (2). Therefore, predicting such range expansion and invasion dynamics is of great interest. However, making ecological predictions is challenging because of the various sources of environmental and demographic stochasticity, along with the complexity intrinsic to biological systems. As a consequence, the uncertainty associated with ecological predictions, given a spatial and temporal scale (3), is large, which implies that predictability tends to be small. For example, even in highly controlled laboratory settings, it is not clear if ecological models can correctly predict range dynamics and the uncertainty associated with them (4, 5).

To make matters even worse, contemporary evolution can not only affect ecological patterns and dynamics (6) but also modify the predictability of range expansions (7). This is because range expansions both drive and are impacted by evolution of traits that influence spatial spread (dispersal ability) and demography (reproduction), forming an eco-evolutionary feedback loop (8). During range expansions, dispersal evolves due to spatial sorting of dispersers (9), whereby faster dispersers end up at the range front, speeding up spread (10). It is therefore not surprising that models including dispersal evolution better predict range expansions, yet, they still globally underpredict their speed (11). In addition, range expansion into heterogeneous environments, such as abiotic gradients of temperature, salinity, or humidity, for example, may greatly be limited by local adaptation to the environmental conditions (12–14). In analogy to dispersal evolution, rapid evolution of local adaptation modifies the demography of the expanding population by changing survivorship or fecundity in the novel environment. Finally, gene surfing, the spatial analog of genetic drift (15), introduces stochasticity due to evolution.

While these challenges have been addressed in the literature, relevant models often assume evolution under equilibrium ecological conditions and focus on optimal phenotypes. During range expansions, however, ecological and evolutionary change happen on similar timescales. Clearly, adaptive evolution in response to rapid ecological changes is contingent on the supply of genetic variation (16). Therefore, one must consider not only evolutionary optima but also the rate of evolutionary change, that is, evolvability. Evolvability of a trait depends on variation, which refers to the standing genetic variation (17) of the trait, and variability (18), which describes the generation of novel genetic variation by means of mutation or recombination (reviewed in ref. 19). While variation can be studied using

Author affiliations: [a]Indian Institute of Science Education and Research Pune, Pune, 411008 Maharashtra, India; and [b]Institut des Sciences de l'Evolution - Montpellier (ISEM), Université de Montpellier, CNRS, IRD, 34095 Montpellier, France

Author contributions: J.N.D. and E.A.F. designed research; J.N.D. and E.A.F. performed research; J.N.D. analyzed data; and J.N.D. and E.A.F. wrote the paper.

The authors declare no competing interest.

This article is a PNAS Direct Submission.

[1]To whom correspondence may be addressed. Email: jhelam-nitin.deshpande@umontpellier.fr or emanuel.fronhofer@umontpellier.fr.

This article contains supporting information online at https://www.pnas.org/lookup/suppl/doi:10.1073/pnas.2121858119/-/DCSupplemental.

Published July 27, 2022.

standard quantitative genetics approaches, the study of variability requires knowledge of numbers and effects of loci, their epistatic interaction, pleiotropy, mutation rates, and mutation effects (18). These properties depend on the genetic architecture (20), or the genotype-to-phenotype map (21–23) of the trait of interest. As a consequence, Melián et al. (24) argue that the structure of gene networks has to be taken into account for an appropriate integration of ecology and evolution.

Despite the relevance of a trait's genetic architecture, eco-evolutionary models of range expansions typically make strong simplifying assumptions regarding the genetic basis of dispersal (25). Some studies of local adaptation during range expansions have assumed more complex additive (26–28) and nonadditive genetic architectures (29, 30). Other studies have tried to understand the impact of ploidy (31) and modifiers of mutation rates (32) on eco-evolutionary range dynamics. Yet, up to now, models of range expansions into environmental gradients have not taken into account the genetic architecture of both relevant traits: dispersal and local adaptation.

One promising way to integrate genetic architecture into models of range expansions is gene-regulatory network (GRN) models, particularly the one introduced by Wagner (33). The GRN genotype-to-phenotype (GP) map consists of a number of transcription factors which can regulate each other's gene expression states. Interactions between genes are represented by a regulatory matrix (the genotype) containing weights. These weights are optimized by evolutionary simulations, where fitness is a function of gene expression levels (phenotype under selection). Some variants of the Wagner model also include an explicit map from gene expression states to a continuous (34) or discrete (35) phenotype, on which fitness then depends. Nonlinearity in the interaction between different loci in the Wagner model and its variants implies that mutation effects are emergent and not fixed as assumed in quantitative genetics models. Therefore, particularly the robustness (decreased sensitivity) to mutation, also known as genetic canalization, has been studied extensively in the Wagner model and its variants (36–39). GRN models have also been used to study the evolution of evolvability under conditions of ecological change (34, 35, 40), including local adaptation (29, 30, 41). Kimbrell (29) showed that local adaptation was accompanied by a transient breakdown of canalization (increased sensitivity to mutation) during a linear four-patch range expansion.

With this background, we seek to address how a microscopic property, such as the genetic architecture of a trait, can modify predictions of large-scale, macroscopic processes, here range expansion dynamics. We develop a stochastic individual-based metapopulation model of range expansions into an environmental gradient (for example, temperature or salinity) in which dispersal and local adaptation traits can evolve and are assumed to result from the products of two noninteracting gene-regulatory networks.

Concretely, we model a metapopulation of a sexually reproducing, diploid species with discrete, nonoverlapping generations. Local population dynamics follow logistic growth. Dispersal is local, and individuals may die with a certain probability during dispersal [μ; dispersal costs (42)]. Initially, the metapopulation adapts to the constant environment in its native habitat (Fig. 1*A*). With this evolutionary history, the species may subsequently expand its range into a linear environmental gradient (Fig. 1*A*). In this gradient, local environmental conditions [$\tau_{env}(x)$] impact the survivorship of a female's offspring. Depending on the mismatch (s) between the female's genetically encoded local adaptation phenotype (τ) and the environment, the offspring's survivorship is reduced following a Gaussian function. Thus, the local adaptation

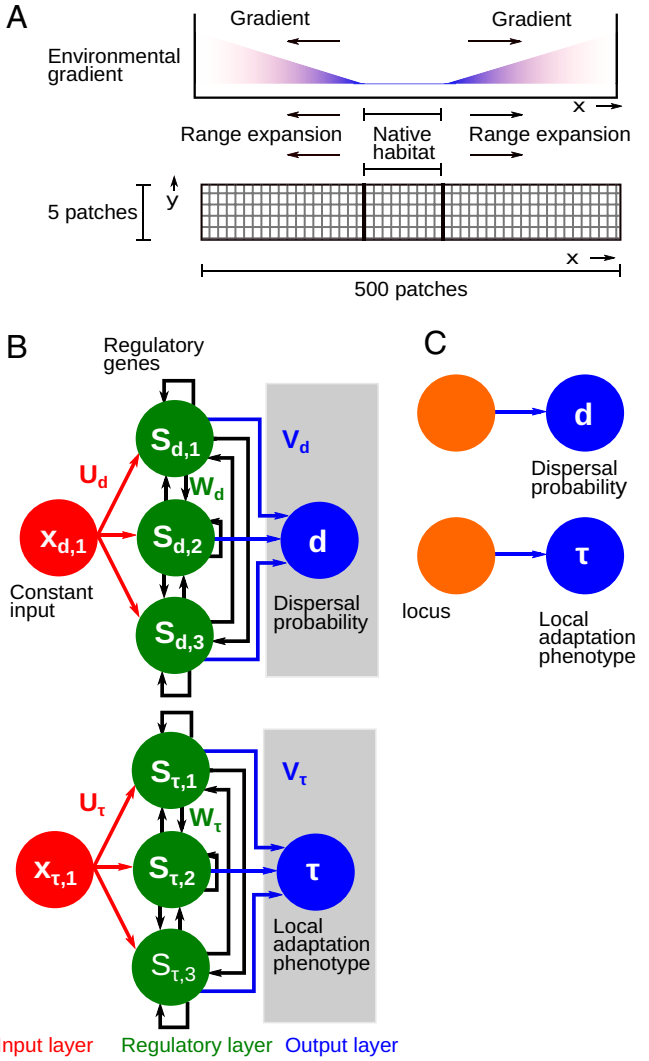

Fig. 1. Range expansions into an environmental gradient (*A*) and the assumed genetic architectures (*B* and *C*). (*A*) We model range expansions into an environmental gradient in a landscape of 500 × 5 patches. Individuals are initially adapted to their constant, native habitat (range core; central 10 × 5 patches) and can subsequently expand their range into a novel linear environmental gradient of slope b along the x direction. Dispersal is local, and individuals may disperse to one of their eight nearest neighbors. In our standard scenario, we compare range expansion dynamics assuming either that dispersal and local adaptation traits result from the products of two noninteracting GRNs (*B*) or that both traits have a simple additive genetic architecture (*C*). (*B*) The GRN model. Two noninteracting GRNs separately encode dispersal probability (d) and the local adaptation phenotype (τ) of a Gaussian niche function. Each GRN has an input layer (constant input $x_{z,1}$ to each gene, where z represents the dispersal trait d or the local adaptation trait τ), a regulatory layer (regulatory genes with expression level $S_{z,i}$ for every gene i for the trait z), and an output layer (the phenotype downstream of gene expression, here dispersal [d] or local adaptation [τ]) highlighted in gray. $\mathbf{U}_z$, $\mathbf{W}_z$, and $\mathbf{V}_z$ are matrices of weights that connect the input layer to the regulatory layer, the genes within the regulatory layer, and map gene expression states to the output phenotype, respectively, for each trait z. (*C*) Simple additive genetic architecture. One quantitative locus each encodes dispersal (d) and the local adaptation trait (τ). Even though in the main text results we assume a simple additive model with only one locus for each trait, we also explore the consequences of assuming different numbers of loci and per locus mutation effects (*SI Appendix*).

phenotype corresponds to the external environment that maximizes female fecundity. Importantly, dispersal (d) and local adaptation (τ) traits are assumed to result from the effects of two noninteracting gene-regulatory networks (GRN model; Fig. 1*B*). A more detailed model description can be found in Fig. 1 and in *SI Appendix*. Parameters are explained in *SI Appendix*, Table S1.

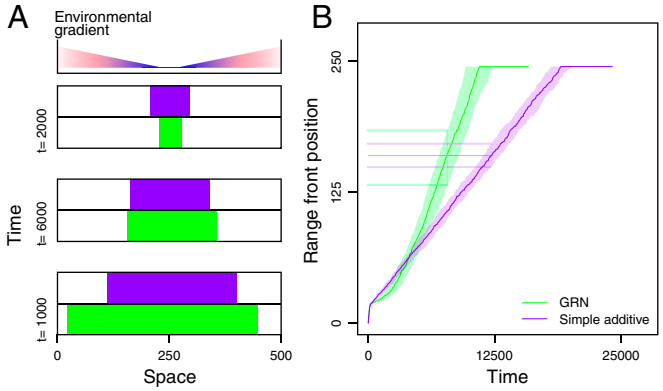

Fig. 2. Comparing range dynamics for GRN (green) and simple additive (purple) genetic architectures. (*A*) Example snapshot of the landscape at different times ($t = 2{,}000$, 6,000, 10,000) since the beginning of range expansion where occupied patches are in color and unoccupied patches are blank. The environmental gradient increases symmetrically on either side of the landscape. Early in the range expansion ($t = 2{,}000$), new patches are colonized more quickly in the simple additive model, but accelerating range expansions in the GRN model invert this pattern later on ($t = 6{,}000$, 10,000). (*B*) Range front position, that is, the position of the occupied patch farthest from the range core, as a function of time since the beginning of range expansion. Since we model a symmetric environmental gradient, range expansions toward both sides of the landscape are comparable. Thus, we pool the 50 replicates, which amount to a total of 100 range expansions. The solid line represents the median position of the range front over these 100 range expansions of our stochastic model. The shading represents the corresponding interquartile range. The horizontal lines highlight the differences in variability of range expansion between the GRN and simple additive models when the range front is at the same median distance (160 patches; indicated in gray) from the range core. Focal scenario parameters are as follows: $b = 0.04$, $\lambda_0 = 2$, $\alpha = 0.01$, $m_{min} = 0.0001$, $\mu = 0.1$, $\epsilon = 0$, $\omega = 1$, and number of genes per GRN $n = 3$.

We compare emergent range dynamics in our GRN model with a complex genetic architecture, to a model in which quantitative loci encode dispersal and local adaptation each (simple additive architecture; Fig. 1*C*). The main difference between these models is that mutational effects, that is, how sensitive a trait is to mutation (41), are emergent in the GRN model but are fixed in the simple additive genetic architecture. While absolute differences in range expansion speeds between the models will depend on the exact per locus mutation effects and number of loci, relaxing the often made assumption of additivity in the GRN model is expected to modify range dynamics qualitatively: evolvability and changing mutation effects in the GRN model may lead to accelerating range dynamics, also making them more variable, or less predictable. Differences in range dynamics could be driven by the genetic architecture of dispersal (rate of spread) or of local adaptation (demography), or both could interact. We analyze the relative importance of dispersal versus local adaptation by developing models with mixed genetic architectures in which dispersal is encoded by a simple additive architecture and local adaptation (LA) by a GRN (GRN LA + simple additive dispersal) and vice versa (simple additive LA + GRN dispersal).

Results and Discussion

We first consider emergent range dynamics focusing on the position of the range front, that is, the farthest occupied patch from the range core, as a function of time since the beginning of the range expansion. We find that the GRN model leads to accelerating range expansion dynamics, when contrasted with the simple additive model (Fig. 2). The acceleration observed in the GRN model is robust to changes in model parameters, that is, for environmental gradients of different steepness (b), changing dispersal costs (μ), and stochastic events such as random patch extinctions (ϵ; *SI Appendix*, Figs. S1 and S2). Importantly, when other additive architectures with differing number of loci and mutation effects are considered, range expansions can be overall faster or slower, depending on the details of these additive architectures, but are not accelerating in comparison to the GRN model (*SI Appendix*, Figs. S3 and S4).

Why do we observe accelerating range expansions in the GRN model but not in the simple additive model? Fundamentally, rapid evolution of either dispersal or of demographic traits during the range expansion process could modify expansion speeds.

Dispersal Evolution. In the absence of an environmental gradient, dispersal evolution has been shown to lead to accelerating range expansions (10, 43). We recapture these accelerating dynamics in the absence of environmental gradients, irrespective of whether dispersal is encoded by a GRN or a simple additive genetic architecture (*SI Appendix*, Fig. S5). Increased dispersal at the range expansion front evolves in both the simple additive and GRN models (Fig. 3*A*) when environmental gradients are present (see also ref. 44). However, dispersal evolves to greater values in the GRN model when compared to the simple additive model.

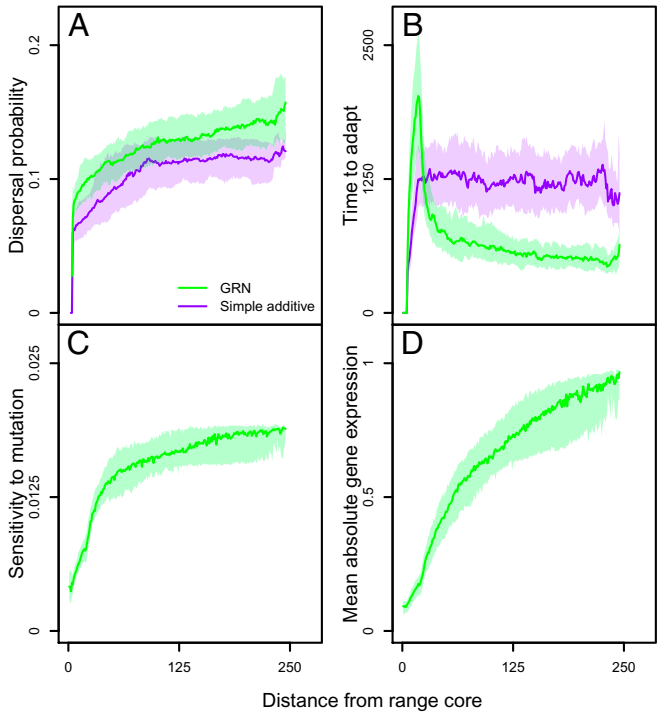

Fig. 3. Evolved dispersal probability (*A*), time to adapt (*B*), sensitivity to mutation (*C*), and mean absolute gene expression levels (*D*) as a function of the distance from the range core for the GRN (green) and simple additive (purple) models. All measures are calculated for 100 replicate range expansions, solid lines are medians, and shaded areas interquartile ranges. (*A*) Dispersal probability increases as the expanding population moves farther from the range core in both the GRN and simple additive models. (*B*) Time to adapt. The time to adapt is the duration an expanding population takes to completely adapt to a novel environment (patch cross-section). The time to adapt decreases as the expanding population moves farther along the environmental gradient for the GRN model but remains constant in the simple additive model. Note that the initial increase is due to standing genetic variation present in the range core. (*C*) Sensitivity to mutation of the local adaptation trait. This is a measure of how much the local adaptation phenotype changes in response to an introduced mutation in the GRN genotype (*SI Appendix*). For the GRN model, the sensitivity to mutation increases as a function of the distance from the range core. Phenotypic effects of mutation cannot change in the simple additive model. (*D*) Mean absolute gene expression. We average the absolute value of gene expression states of all genes in the GRN. Gene expression states evolve to extremes farther away from the range core. Focal scenario parameters are as follows: $b = 0.04$, $\lambda_0 = 2$, $\alpha = 0.01$, $m_{min} = 0.0001$, $\mu = 0.1$, $\epsilon = 0$, $\omega = 1$, and number of genes per GRN $n = 3$.

To test whether differences in dispersal genetic architecture, and hence dispersal evolution, drive accelerating range dynamics in the GRN model, we use our mixed genetic architecture models and show that accelerating range expansions into environmental gradients occur only when the local adaptation trait is encoded by a GRN, irrespective of the genetic architecture of dispersal (*SI Appendix*, Figs. S6 and S7). Even when dispersal does not evolve, a GRN genetic architecture for local adaptation leads to accelerating range expansions (*SI Appendix*, Figs. S8 and S9). However, dispersal evolution does increase the overall speed of range expansion relative to when dispersal is fixed (*SI Appendix*, Figs. S8 and S9). Thus, the GRN genetic architecture of dispersal does not drive accelerating range expansion dynamics in our model.

Evolution of Local Adaptation. As a consequence, as soon as environmental gradients are present, which is very likely the case in nature (e.g., climatic gradients) (45), our model suggests that dispersal evolution, and the ability of individuals at the expansion front to spread, may not be the main driver of accelerating range expansions. Therefore, acceleration along gradients must be due to changes in traits that rather impact demography directly by limiting population growth in novel environments, which in our study implies evolution of local adaptation.

In order to better understand the dynamics of local adaptation, we follow the time a population needs to adapt to the conditions in a patch across the gradient (here defined as level of adaptation $s > 0.96$) and refer to this as the "time to adapt." The time to adapt for the simple additive model does not change as the population expands along the gradient (Fig. 3*B*). However, in the GRN model, the farther away a patch is from the range core, the smaller the time to adapt (Fig. 3*B*). This means that as the population moves along the environmental gradient, it adapts more quickly to new local conditions (for representative dynamics of local adaptation in both models, see *SI Appendix*, Fig. S10).

Why does the time to adapt decrease in the GRN model? In other words, why does the rate of adaptation increase in the GRN model but remain constant in the simple additive model? One crucial difference between the assumptions of the GRN model and the simple additive model is how mutations change the phenotype, that is, the sensitivity to mutation. If a mutation is introduced into one of the alleles encoding local adaptation in the simple additive model, the phenotype will change linearly with this mutation. However, in the GRN model, the sensitivity to mutation can itself evolve because of nonlinearity in the interaction between the multiple loci. Here the sensitivity to mutation increases in a saturating manner as the population moves farther along the gradient and away from the range core (Fig. 3*C*). This increased sensitivity to mutation allows the expanding populations to adapt more quickly and reduces the time until a given population is fully adapted (*SI Appendix*, Figs. S10 and S11). Interestingly, our model predicts that increased sensitivity to mutation is accompanied by the evolution of extreme gene expression levels (Fig. 3*D*).

This association of extreme gene expression states with a greater sensitivity to mutation is an interesting consequence of assuming a mapping between equilibrium gene expression states and the phenotype under selection, here a continuous local adaptation trait. Indeed, such an association is contrary to the expectation from the Wagner model (33) with sigmoid gene expression (37). Rünneburger and Le Rouzic (39) have shown that in such a model, stabilizing selection on discrete gene expression states that are closer to the extremes of the sigmoid (-1 or 1) lead to more canalized (less sensitive) GRNs (Fig. 4*A*). However, in our

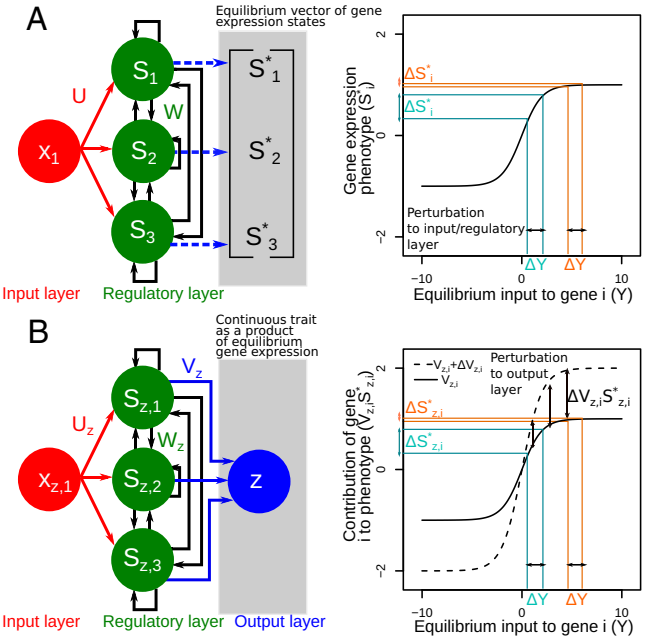

Fig. 4. Mechanism for the evolution of increased sensitivity to mutation in the sigmoid Wagner model (*A*) and the local adaptation GRN in the present study (*B*). For this example, we consider a highly simplified scenario in which the GRN is at a fixed point equilibrium, and we focus on how a single gene would respond to perturbations to the genotype at extreme and intermediate gene expression levels. We further assume that any perturbation in the input the gene receives takes its gene expression to another fixed point equilibrium. For an easier comparison of both GRN models, the phenotype under selection is highlighted with a gray background. (*A*) In the sigmoid Wagner model, the vector of equilibrium gene expression states $\mathbf{S}^*$ is the phenotype under selection; therefore, any perturbation ΔY in the input a single gene receives (either from the input layer or from other genes) would lead to greater phenotypic difference at intermediate gene expression states when compared to those at extremes (ΔS_i^*) (39). (*B*) In our model the output z of the GRN is the continuous local adaptation phenotype under selection. Here the linear effects downstream of a gene i contribute to a trait determined by the output weight $V_{z,i}$; therefore, the contribution of each gene to the phenotype is $V_{z,i}S_{z,i}^*$. In this case, any perturbation in the output weights $V_{z,i}$, say, $V_{z,i} + \Delta V_{z,i}$, would yield a greater difference in contribution to the phenotype at extreme rather than intermediate gene expression.

model, we have assumed a linear mapping between equilibrium gene expression states and the phenotype under selection ($z = \tau$; $z = \sum_{i=1}^{n} V_{z,i} S_{z,i}^*$). Thus, when the expression level for a given gene at equilibrium $S_{z,i}^*$ is closer to the extremes (-1 or 1), any perturbation $\Delta V_{z,i}$ in the corresponding output weight $V_{z,i}$ will be amplified (Fig. 4*B*). Vice versa, closer to intermediate gene expression levels (closer to 0), the perturbation will be silenced. As a consequence, as gene expression states evolve to their extremes, the mutation effects due to a perturbation $\Delta V_{z,i}$ in the output weights become equivalent to mutation effects in a simple additive model with n loci. At the macroscopic level of range expansions, this implies that expansion speeds (slopes in *SI Appendix*, Figs. S3 and S4) and time to adapt to novel environments (*SI Appendix*, Fig. S12) of the GRN and the simple additive model with $n = 3$ loci converge because of decanalization in the GRN model. Importantly, only the GRN model can exhibit changes in sensitivity and therefore changes in range expansion speed which leads to accelerating expansions.

Predictability of Range Expansions. Finally, we investigate how genetic architecture impacts the variation between range expansion replicates and, thereby, predictability sensu Melbourne and Hastings (4). Generally speaking, the GRN model leads not only to accelerating (*SI Appendix*, Figs. S1 and S2) but also to more variable range expansions when compared to the simple

additive model (Fig. 2*B* and *SI Appendix*, Figs. S13 and S14), as can be seen when comparing differences between the left and right range fronts in the GRN model in Fig. 2*A*, for example. Even additive models with $n = 3$ loci, which, as discussed above, have the same per locus mutation effects as the GRN model after decanalization, show less between replicate variation in range expansion dynamics when compared to the GRN model (*SI Appendix*, Figs. S15 and S16). This holds true for different gradient slopes, dispersal costs, and extinction probabilities, irrespective of the genetic architecture assumed for the dispersal trait. The greater variability of range expansions in the GRN model implies that range expansions are less predictable when the GRN encodes local adaptation. This shows that the assumed genetic architecture not only leads to systematically and qualitatively different predictions on average but also to different uncertainties.

General Discussion

Our study highlights the central role of genetic architecture in determining the dynamics of range expansions into an environmental gradient. We show that assuming a complex GRN genetic architecture for relevant traits leads to accelerating range expansions when compared to models that assume a simple additive genetic architecture.

Accelerating range dynamics result from a faster rate of adaptation due to an increase in the sensitivity to mutation of the local adaptation trait, as the expanding population moves along the gradient. As shown by our comparison of alternative models, the genetic architecture of the dispersal trait and even dispersal evolution altogether are not responsible for the acceleration. Rather, the acceleration pattern is exclusively linked to the genetic architecture of local adaptation. The increasing rate of adaptation resulting from evolution of greater sensitivity to mutation in the local adaptation GRN observed in our model is an instance of the evolution of evolvability. Particularly, as defined by Wagner and Altenberg (18), there is a change in trait variability (potential to vary; sensitivity to mutation) in the direction of adaptive opportunity. Cobben et al. (32) have demonstrated the evolution of evolvability in individual-based simulations of range expansion when dispersal, local adaptation, and mutation rates evolve. They find that the rate of adaptation at the range front increases because of the evolution of increased mutation rates encoded by a modifier locus. For sexual species, this result can be sensitive to the assumed distribution of mutation effects and level of linkage between the modifier locus and local adaptation locus because the modifier locus evolves by hitchhiking (46). However, in our model, there is no need for evolution at a modifier locus. Rather, the increase in the rate of adaptation results from the interaction between genes and their downstream effects.

The consideration of mutational effects is important for understanding the rate of adaptation to a gradient landscape, especially in the absence of standing genetic variation. This has been demonstrated in studies of additive genetic architectures: Schiffers et al. (26) find that the rate of adaptation is greatest when the mutational effect size matches the steepness of an environmental gradient. Gilbert and Whitlock (27) show that adaptation to a novel habitat patch proceeds primarily by mutations of large effects. By modeling local adaptation as a GRN, we allow for changes in the sensitivity to mutation itself. As a consequence, whereas in the additive architecture studies described above, mutational effects are fixed parameters, in our work, they are emergent properties. Therefore, while we reemphasize the importance of understanding mutation effects, we add to previous work by showing that the sensitivity to mutation increases as an expanding population moves farther along the gradient, which leads to an increase in the rate of adaptation. This is only possible if the assumption of additivity is relaxed, like in the present study.

Kimbrell (29) and Kimbrell and Holt (41) have shown for a GRN model of local adaptation in a source–sink system, in which gene expression states are the phenotype under selection, that canalization breakdown (increase in sensitivity) is followed by adaptation to a sink or gradient of sinks, with a return to preadaptation levels of canalization. In our model, we show that sensitivity to mutation also increases when the trait under consideration is continuous, resulting from linear downstream effects of a GRN, however, by a different mechanism. In continuous, sigmoid Wagner-like GRN models (37) where gene expression states are the phenotype under selection (including refs. 29 and 41), Rünneburger and Le Rouzic (39) show that selection for extremes of gene expression leads to greater canalization in genes under selection.

By contrast, in our model, we show that greater mutational sensitivity is associated with extremes of gene expression because of the amplification of mutational effects downstream of gene expression. This effect cannot emerge in most GRN models due to the assumption that gene expression states are the phenotype under selection. To our knowledge, this association of sensitivity and extreme gene expression has been discussed only once before by Draghi and Whitlock (47) but with a different kind of GRN model in the context of the evolution of robustness to intrinsic noise. These authors study a trade-off between the robustness of a single gene and a GRN to intrinsic noise (which is greater at low gene expression) and the amplification of mutations in downstream effects (which is greater at high gene expression) and find that robustness to intrinsic noise evolves despite this constraint. Our finding that increased sensitivity to mutation is driven by extremes of gene expression is an interesting prediction going beyond what our model had originally been designed to predict. Concretely, this yields empirically testable predictions for gene expression states under directional selection, namely, that increased sensitivity to mutation should be associated with intermediate gene expression when gene expression states are the phenotype under selection while we predict the opposite to be true for traits that result from effects of gene expression, such as in our model.

Our model assumes a particular genetic architecture underlying dispersal and local adaptation traits. However, our results are likely valid more generally for mutation-limited quantitative trait evolution under directional selection: our proposed mechanism for the evolution of increased sensitivity is not restricted to GRN GP maps but can also emerge in other genetic architectures such as the multilinear GP map. The amplification of downstream mutations by extreme gene expression can be considered as a special case of positive directional epistasis, in which multiple loci interact to amplify each other's effects in the direction of selection. This is a mechanism that has been shown to lead to greater evolvability (48, 49) in a multilinear GP map (50). Hence, we may expect accelerating range expansions in general for nonadditive GP maps.

Our study demonstrates the consequences of relaxing the assumption of additivity and the utility of GRN GP maps for understanding adaptation during range expansions and eco-evolutionary dynamics more generally. However, several open questions remain. Particularly, constraints to the increased sensitivity to mutation imposed by a fixed epistatic structure (48), interactions between multiple traits (34), numbers of genes that contribute directly to the local adaptation phenotype (39), and the evolution of robustness to intrinsic noise (47), to name but a few, would impact range expansion dynamics and represent interesting future avenues of research. Further, by assuming a mapping

between gene expression states and a continuous phenotype trait, we have highlighted how gene expression states themselves might impact evolvability, opening up the question of how various gene expression activation functions and mappings between equilibrium gene expression states and discrete (35) or continuous (34) phenotype under selection might modulate evolvability.

Interestingly, we also find that as long as the local adaptation trait is encoded by a GRN, we observe accelerating range expansions regardless of the genetic architecture underlying the dispersal trait and even in the absence of dispersal evolution. In the absence of environmental gradients, evolution of greater dispersal as a result of spatial sorting (10), spatial selection, and increased kin competition (43) leads to accelerating range expansions. However, when an environmental gradient is present, these advantages of dispersal are greatly reduced by the direct reduction in fitness resulting from maladaptation to the external environment (44). This explains the reduced importance of dispersal genetic architecture in our study. At the same time, this cost–benefit balance also explains why in our GRN model dispersal evolves to higher values during range expansions (Fig. 3*A*): as expanding populations adapt more quickly to the gradient in the GRN model, and therefore reduce maladaptation, spatial selection becomes again more important and leads to higher evolved dispersal probabilities.

Finally, we show that genetic architecture has an important impact on the predictability of range expansions. Between-replicate variation is higher when local adaptation is encoded by a GRN than by a simpler genetic architecture. Therefore, range expansions are less predictable in the GRN model. This could be because in the GRN model, uncertainty is propagated between the process of increase in sensitivity to mutation (evolvability) and adaptation to the new environmental conditions (evolution). The challenges of predicting biological responses to environmental change, in general, are compounded by the levels of organization and spatiotemporal scales (3). In particular, previous purely ecological studies of range expansion have found that stochastic models may either accurately estimate (5) or overestimate (4) the predictability of observed range expansion speeds. Evolution clearly plays a role in the predictability of range expansion (7). We here show that the predictability of range expansions is not only modified by evolution but also by the evolution of evolvability. This finding has two important implications: First, in biological systems in which local adaptation is encoded by a GRN, range expansion and invasion dynamics may be even more variable than predicted using classical models. Second, vice versa, while range expansions may be intrinsically very variable, using appropriate models based on realistic genetic architectures may help to generate accurate predictions of uncertainty. The latter are important as they define the forecast horizon (3) as well as risk management strategies. More generally, our work highlights how assumptions related to microscopic levels of biological organization, here the assumed genetic architecture, can propagate and impact not only mean predictions of eco-evolutionary processes but also their predictability at macroscopic scales.

Materials and Methods

We develop an individual-based metapopulation model of range expansion into a linear external environmental gradient with slope b (*SI Appendix*, Eq. **S3**) in which dispersal and local adaptation traits are encoded by gene-regulatory networks (Fig. 1). A summarized model description is given below, and details can be found in *SI Appendix*.

Life Cycle. We assume a diploid organism that reproduces sexually. Dispersal is natal and costly (dispersal costs μ) and, since the landscape is represented by a regular grid, possible to the eight nearest-neighboring patches. Individuals disperse according to a genetically encoded dispersal probability d which is either represented by a GRN or a single quantitative locus (Fig. 1*B* and *C*). After dispersal, individuals may reproduce in their target patches. Local population dynamics follow the Beverton–Holt model of discrete logistic growth (*SI Appendix*, Eq. **S1**). A female chooses a mate at random from its own patch.

The realized expected fecundity of a female is modified by the environment following a Gaussian niche function (*SI Appendix*, Eq. **S4**; local adaptation phenotype τ). The number of offspring a female produces is Poisson distributed with a mean equal to its realized fecundity in order to capture demographic stochasticty. For all genetic architectures explored, offspring inherit parental genotypes, one allele from the female and male parent at each locus. After reproduction, the parental generation dies and is replaced by the offspring generation. Entire patches may go extinct with a probability ϵ representing random catastrophic patch extinction events.

Genetic Architecture. A detailed description of the GRN model and other alternate genetic architectures can be found in *SI Appendix*.

GRN genetic architecture. As shown in Fig. 1*B*, we model the GRN for each trait (indexed by $z = d, \tau$) as having three layers: input layer, regulatory layer, and output layer (35).

We represent the expression states of the regulatory genes by $\mathbf{S}_z(l)$ for each modeled trait $z = d, \tau$ at the lth iteration of a developmental process (33). Gene expression states at each iteration during development are continuous and sigmoid functions of the input they receive and may take values between -1 and 1 (37). The slope ($\mathbf{r}_z$) and threshold ($\boldsymbol{\theta}_z$) of this sigmoid are properties of the regulatory genes and are genetically encoded (35). Each gene receives a single constant input. The input matrix ($\mathbf{U}_z$) connects the input layer to the regulatory layer. The regulatory genes influence each other's expression states according to weights present in a genetically encoded regulatory matrix ($\mathbf{W}_z$). The dynamical developmental process (*SI Appendix*, Eq. **S5**) takes place for 20 iterations for each individual, and the equilibrium gene expression states ($\mathbf{S}_z^*$) characterize the developmental system if a fixed point steady state is reached within this duration (34). Limit cycle dynamics are not considered viable (33).

Finally, we assume that the trait under consideration varies linearly with equilibrium gene expression states. As a consequence, each trait is given by the weighted sum (*SI Appendix*, Eq. **S6**) of the gene expression levels (34), and the output matrix ($\mathbf{V}_z$) is composed of these weights. Thus, the output layer processes the gene expression states and gives the trait. The input matrix, regulatory matrix, and output matrix along with the threshold and slope of the sigmoid are genetically encoded by diploid loci. These loci are initialized randomly using a Gaussian distribution with mean 0 and SD 1 and are subject to mutation with a probability $m(t)$ (*SI Appendix*, Eq. **S2** and Table S1) and effects drawn from a normal distribution with SD 0.1.

Simple additive genetic architecture. In the simple additive model, one diploid quantitative locus each encodes dispersal probability (d) and the local adaptation phenotype (τ) to local adaptation (Fig. 1*C*). Each allele for a given locus is initialized with a random number drawn from a uniform distribution going from 0 to 1. Alleles may mutate during inheritance with a given probability m_{min} (*SI Appendix*, Eq. **S2** and Table S1) and by a number drawn from a normal distribution with mean 0 and SD 0.1.

Analysis. For all the parameter combinations explored (*SI Appendix* and *SI Appendix*, Table S1), we ran 50 replicate simulations, which amounts to 100 range expansions (left and right sides of the expanding metapopulation), and tracked the range border position as a function of time. For the focal scenario, we also track the average dispersal probability, level of adaptation (s), the sensitivity to mutation (for details, see *SI Appendix*), and the gene expression states of the local adaptation GRN throughout the landscape. The sensitivity to mutation is a measure of how much a trait changes if the GRN is perturbed.

Additionally, we calculate the time to adapt, which is the difference between the time when the expanding population enters a given patch cross-section and the time when the population adapts to it completely. We use a threshold for the level of adaptation $s > 0.96$ because the population cannot reach $s = 1$ as a consequence of expansion or genetic load.

Data Availability. Computer code is available at GitHub and Zenodo (DOI: 10.5281/zenodo.5747752) (51).

ACKNOWLEDGMENTS. We thank two anonymous referees for very helpful comments. This work was supported by a grant from the Agence Nationale de la Recherche (Grant ANR-19-CE02-0015) to E.A.F. This is publication ISEM-2022-160-SUD of the Institut des Sciences de l'Evolution–Montpellier.

1. J. M. Bullock *et al.*, Human-mediated dispersal and the rewiring of spatial networks. *Trends Ecol. Evol.* **33**, 958–970 (2018).
2. I. C. Chen, J. K. Hill, R. Ohlemüller, D. B. Roy, C. D. Thomas, Rapid range shifts of species associated with high levels of climate warming. *Science* **333**, 1024–1026 (2011).
3. O. L. Petchey *et al.*, The ecological forecast horizon, and examples of its uses and determinants. *Ecol. Lett.* **18**, 597–611 (2015).
4. B. A. Melbourne, A. Hastings, Highly variable spread rates in replicated biological invasions: Fundamental limits to predictability. *Science* **325**, 1536–1539 (2009).
5. A. Giometto, A. Rinaldo, F. Carrara, F. Altermatt, Emerging predictable features of replicated biological invasion fronts. *Proc. Natl. Acad. Sci. U.S.A.* **111**, 297–301 (2014).
6. L. Govaert *et al.*, Eco-evolutionary feedbacks–Theoretical models and perspectives. *Funct. Ecol.* **33**, 13–30 (2019).
7. J. L. Williams, R. A. Hufbauer, T. E. X. Miller, How evolution modifies the variability of range expansion. *Trends Ecol. Evol.* **34**, 903–913 (2019).
8. T. E. X. Miller *et al.*, Eco-evolutionary dynamics of range expansion. *Ecology* **101**, e03139 (2020).
9. R. Shine, G. P. Brown, B. L. Phillips, An evolutionary process that assembles phenotypes through space rather than through time. *Proc. Natl. Acad. Sci. U.S.A.* **108**, 5708–5711 (2011).
10. B. L. Phillips, G. P. Brown, J. K. Webb, R. Shine, Invasion and the evolution of speed in toads. *Nature* **439**, 803–803 (2006).
11. T. A. Perkins, B. L. Phillips, M. L. Baskett, A. Hastings, Evolution of dispersal and life history interact to drive accelerating spread of an invasive species. *Ecol. Lett.* **16**, 1079–1087 (2013).
12. M. Kirkpatrick, N. H. Barton, Evolution of a species' range. *Am. Nat.* **150**, 1–23 (1997).
13. G. García-Ramos, D. Rodríguez, Evolutionary speed of species invasions. *Evolution* **56**, 661–668 (2002).
14. M. Szűcs *et al.*, Rapid adaptive evolution in novel environments acts as an architect of population range expansion. *Proc. Natl. Acad. Sci. U.S.A.* **114**, 13501–13506 (2017).
15. M. Slatkin, L. Excoffier, Serial founder effects during range expansion: A spatial analog of genetic drift. *Genetics* **191**, 171–181 (2012).
16. H. Kokko *et al.*, Can evolution supply what ecology demands? *Trends Ecol. Evol.* **32**, 187–197 (2017).
17. D. Houle, Comparing evolvability and variability of quantitative traits. *Genetics* **130**, 195–204 (1992).
18. G. P. Wagner, L. Altenberg, Perspective: Complex adaptations and the evolution of evolvability. *Evolution* **50**, 967–976 (1996).
19. M. Pigliucci, Is evolvability evolvable? *Nat. Rev. Genet.* **9**, 75–82 (2008).
20. T. F. Hansen, The evolution of genetic architecture. *Annu. Rev. Ecol. Evol. Syst.* **37**, 123–157 (2006).
21. P. Alberch, From genes to phenotype: Dynamical systems and evolvability. *Genetica* **84**, 5–11 (1991).
22. M. Pigliucci, Genotype-phenotype mapping and the end of the 'genes as blueprint' metaphor. *Philos. Trans. R. Soc. Lond. B Biol. Sci.* **365**, 557–566 (2010).
23. D. Nichol, M. Robertson-Tessi, A. R. A. Anderson, P. Jeavons, Model genotype-phenotype mappings and the algorithmic structure of evolution. *J. R. Soc. Interface* **16**, 20190332 (2019).
24. C. J. Melián *et al.*, Deciphering the interdependence between ecological and evolutionary networks. *Trends Ecol. Evol.* **33**, 504–512 (2018).
25. M. Saastamoinen *et al.*, Genetics of dispersal. *Biol. Rev. Camb. Philos. Soc.* **93**, 574–599 (2018).
26. K. Schiffers *et al.*, Landscape structure and genetic architecture jointly impact rates of niche evolution. *Ecography* **37**, 1218–1229 (2014).
27. K. J. Gilbert, M. C. Whitlock, The genetics of adaptation to discrete heterogeneous environments: Frequent mutation or large-effect alleles can allow range expansion. *J. Evol. Biol.* **30**, 591–602 (2017).
28. K. J. Gilbert *et al.*, Local adaptation interacts with expansion load during range expansion: Maladaptation reduces expansion load. *Am. Nat.* **189**, 368–380 (2017).
29. T. Kimbrell, Canalization and adaptation in a landscape of sources and sinks. *Evol. Ecol.* **24**, 891–909 (2010).
30. J. W. Malcom, Gene networks and metacommunities: Dispersal differences can override adaptive advantage. *PLoS One* **6**, e21541 (2011).
31. A. Kubisch, R. D. Holt, H. J. Poethke, E. A. Fronhofer, Where am I and why? Synthesizing range biology and the eco-evolutionary dynamics of dispersal. *Oikos* **123**, 5–22 (2014).
32. M. M. P. Cobben, O. Mitesser, A. Kubisch, Evolving mutation rate advances the invasion speed of a sexual species. *BMC Evol. Biol.* **17**, 150 (2017).
33. A. Wagner, Evolution of gene networks by gene duplications: A mathematical model and its implications on genome organization. *Proc. Natl. Acad. Sci. U.S.A.* **91**, 4387–4391 (1994).
34. J. A. Draghi, M. C. Whitlock, Phenotypic plasticity facilitates mutational variance, genetic variance, and evolvability along the major axis of environmental variation. *Evolution* **66**, 2891–2902 (2012).
35. J. van Gestel, F. J. Weissing, Regulatory mechanisms link phenotypic plasticity to evolvability. *Sci. Rep.* **6**, 24524 (2016).
36. A. Wagner, Does evolutionary plasticity evolve? *Evolution* **50**, 1008–1023 (1996).
37. M. L. Siegal, A. Bergman, Waddington's canalization revisited: Developmental stability and evolution. *Proc. Natl. Acad. Sci. U.S.A.* **99**, 10528–10532 (2002).
38. S. Ciliberti, O. C. Martin, A. Wagner, Innovation and robustness in complex regulatory gene networks. *Proc. Natl. Acad. Sci. U.S.A.* **104**, 13591–13596 (2007).
39. E. Rünneburger, A. Le Rouzic, Why and how genetic canalization evolves in gene regulatory networks. *BMC Evol. Biol.* **16**, 239 (2016).
40. J. Draghi, G. P. Wagner, The evolutionary dynamics of evolvability in a gene network model. *J. Evol. Biol.* **22**, 599–611 (2009).
41. T. Kimbrell, R. D. Holt, Canalization breakdown and evolution in a source-sink system. *Am. Nat.* **169**, 370–382 (2007).
42. D. Bonte *et al.*, Costs of dispersal. *Biol. Rev. Camb. Philos. Soc.* **87**, 290–312 (2012).
43. A. Kubisch, E. A. Fronhofer, H. J. Poethke, T. Hovestadt, Kin competition as a major driving force for invasions. *Am. Nat.* **181**, 700–706 (2013).
44. M. Andrade-Restrepo, N. Champagnat, R. Ferrière, Local adaptation, dispersal evolution, and the spatial eco-evolutionary dynamics of invasion. *Ecol. Lett.* **22**, 767–777 (2019).
45. R. I. Colautti, S. C. H. Barrett, Rapid adaptation to climate facilitates range expansion of an invasive plant. *Science* **342**, 364–366 (2013).
46. D. Romero-Mujalli, F. Jeltsch, R. Tiedemann, Elevated mutation rates are unlikely to evolve in sexual species, not even under rapid environmental change. *BMC Evol. Biol.* **19**, 175 (2019).
47. J. Draghi, M. Whitlock, Robustness to noise in gene expression evolves despite epistatic constraints in a model of gene networks. *Evolution* **69**, 2345–2358 (2015).
48. A. J. R. Carter, J. Hermisson, T. F. Hansen, The role of epistatic gene interactions in the response to selection and the evolution of evolvability. *Theor. Popul. Biol.* **68**, 179–196 (2005).
49. T. F. Hansen, J. M. Álvarez Castro, A. J. R. Carter, J. Hermisson, G. P. Wagner, Evolution of genetic architecture under directional selection. *Evolution* **60**, 1523–1536 (2006).
50. T. F. Hansen, G. P. Wagner, Modeling genetic architecture: A multilinear theory of gene interaction. *Theor. Popul. Biol.* **59**, 61–86 (2001).
51. J. N. Deshpande, E. A. Fronhofer, Code associated with Deshpande & Fronhofer 2022 PNAS. Zenodo. https://doi.org/10.5281/zenodo.5747752. Deposited 1 December 2021.